Optical evidence for a change in the heavy electron Fermi surface at a magnetic quantum critical point of $CeNi_{1-x}Co_xGe_2$

2008 J. Phys.: Condens. Matter 20 285202

(http://iopscience.iop.org/0953-8984/20/28/285202)

J. Phys.: Condens. Matter **20** (2008) 285202 (5pp) doi:10.1088/0953-8984/20/28/285202

Optical evidence for a change in the heavy electron Fermi surface at a magnetic quantum critical point of $CeNi_{1-x}Co_xGe_2$

K E Lee[1], C I Lee[1], H J Oh[1,2], H J Im[1], Tuson Park[1], S Kimura[3] and Y S Kwon[1,4]

[1] Department of Physics, Sungkyunkwan University, Suwon 440-746, Korea
[2] Department of Ophthalmic Optics, Masan College, Masan 630-729, Korea
[3] UVSOR Facility, Institute for Molecular Science, Okazaki 444-8585, Japan
[4] Center for Strongly Correlated Material Research, Seoul National University, Seoul 151-742, Korea

E-mail: yskwon@skku.ac.kr

Received 5 March 2008, in final form 5 May 2008
Published 13 June 2008
Online at stacks.iop.org/JPhysCM/20/285202

Abstract

Optical properties of $CeNi_{1-x}Co_xGe_2 (0 \leqslant x \leqslant 1)$ have been studied via infrared spectroscopy. Tuning the Co-doping concentration reveals clear demarcation in the optical properties at $x = 0.3$, where non-Fermi liquid behavior appears. For $x > 0.3$, a hump in the optical conductivity σ_1 is observed at about 0.2 eV, resulting from strong hybridization between conduction electrons and Ce 4f electronic states. For $x \leqslant 0.3$, in contrast, no such hump is observed. The low frequency plasmon observed below the coherence temperature T^* for $x > 0.3$ is also consistent with the existence of heavy quasiparticles. These dramatic changes in the optical response at $x = 0.3$ indicate that the heavy electron Fermi surface of $CeNi_{1-x}Co_xGe_2$ ($x > 0.3$) ceases to exist at this magnetic quantum critical point.

(Some figures in this article are in colour only in the electronic version)

Recent interest on quantum effects has been intensified from the perspective of its relevance to unconventional superconductivity, especially in high-T_c copper oxides and heavy fermion superconductors [1, 2]. Heavy fermion metals, where strong correlation effects make the effective mass two or three orders of magnitude larger than the bare electron mass, have provided fertile ground in exploring and understanding the nature of quantum critical matter or non-Fermi liquid behavior arising from the continuous quantum phase transition. Neutron scattering measurements on $CeCu_{6-x}Au_x$ exhibited localized-spin excitations in the quantum critical regime [3], unanticipated from conventional spin-density wave description [4]. Si *et al* proposed a locally critical quantum phase transition where local fluctuations from the local moments become critical simultaneously [5]. One of the consequences of this model is a sudden change in the Fermi surface at the critical point due to the inclusion of f-electrons into conduction bands. Hall effect measurements of the field-tuned quantum critical metal $YbRh_2Si_2$ indicated a rapid change in the Hall coefficient [6], suggesting an abrupt change in the Fermi surface. Recently, de Haas–van Alphen (dHvA) measurements of the pressure-tuned heavy fermion superconductor $CeRhIn_5$ suggested a Fermi volume expansion at a critical pressure where the antiferromagnetic transition temperature is suppressed to zero temperature [2, 7].

Infrared spectroscopy is an ideal probe to explore Fermi volume change when a magnetic ground state changes to a non-magnetic heavy fermion state via a quantum critical point (QCP). In heavy fermion metals, a hybridization gap is formed below the coherence temperature T^* due to strong coupling between localized f-electrons and conduction electrons. Since the hybridization gap can be directly measured as absorption in optical conductivity, systematic studies on the hybridization gap in the vicinity of the QCP will provide essential information on the nature of quantum criticality, especially distinguishing the conventional spin-density type [4] and the localized-spin fluctuations scenario [5]. Isostructural Co-doped Ce compounds $CeNi_{1-x}Co_xGe_2$ are best suited to this

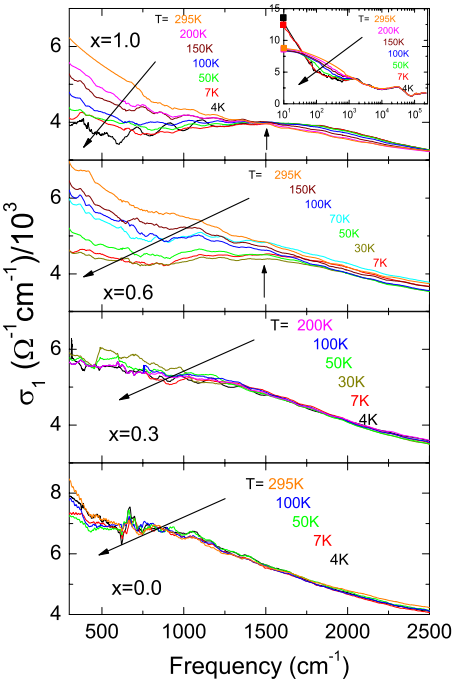

Figure 1. Real part of optical conductivity in the infrared region for $CeNi_{1-x}Co_xGe_2$ ($x = 1.0, 0.6, 0.5, 0.3$ and 0.0) at selected temperatures. Insets depict the real part of optical conductivity in the whole measured optical range. The symbols on the left axis of the inset represent dc values at different temperatures.

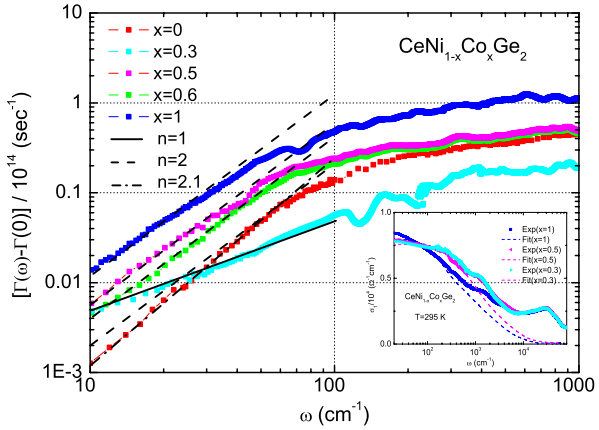

Figure 2. Frequency dependence of the scattering rate in the low frequency regions at $T = 4$ K for $x = 1$, 0.3 and 0, and at $T = 7$ K for $x = 0.5$ and 0.6. $\Gamma(0)$ is the scattering rate value at $\omega = 0$. n represents the ω^n-dependence of the scattering rate. The inset shows the Drude fitting for $x = 1$, 0.6 and 0.5 at 295 K. The plasma frequency for three samples are nearly the same as 2.9 eV.

purpose because the ground state varies from antiferromagnetic to heavy fermion states via an AFM quantum critical point at $x = 0.3$ and the lattice volume is essentially unchanged with Co concentration, suggesting that there is electronic tuning of the ground states [8]. In this Letter, we report optical properties of $CeNi_{1-x}Co_xGe_2$ in the complete range of $x = 0$ through $x = 1$, where a hump feature corresponding to hybridization gap is observed below the coherence temperature T^* in the real part of optical conductivity and T^*, which is similar to T_R^* determined from electrical resistivity, is undetectable down to the lowest measuring temperature near $x = 0.3$. The results are consistent with the collapse of the heavy electron Fermi surface at the quantum critical point.

Polycrystalline samples of $CeNi_{1-x}Co_xGe_2$ were prepared by arc melting under an argon atmosphere and annealed at 900 °C for three weeks in an evacuated quartz tube. Near normal incidence reflectivity was performed using a Fourier interferometer from 60 (7 meV) to 12 000 cm^{-1} (1.5 eV) from room temperature to 4 K. Reflectivity at a higher frequency region up to 242 000 cm^{-1} (30 eV) was measured at room temperature in an ultraviolet synchrotron orbital radiation facility (UVSOR) to estimate optical conductivity ($\sigma_1(\omega)$) through Kramers–Kronig analysis, which was also used to obtain σ_1 at low temperatures because the reflectivity at this range is almost independent of temperature. In the energy range below 60 cm^{-1} reflectivity was extrapolated by a modified Hagen–Rubens function: $R(\omega) = 1 - (2\omega/\pi\sigma_{dc})^{1/2} + A\omega$. Here, σ_{dc} is a dc conductivity and A is a fitting parameter for matching between the calculated and measured reflectivity values. Above 242 000 cm^{-1}, reflectivity was extrapolated by $R \propto \omega^4$. Samples were carefully polished with acetone as a lubricant in order to prevent oxidization from the reactive Ce element, and mounted in a circulating He cryostat, where reflectivity measurements were performed without breaking vacuum. Evaporated Au film was mounted next to the sample for reference.

Figure 1 representatively shows the dissipative part of the optical conductivity ($\sigma_1(\omega)$) of $CeNi_{1-x}Co_xGe_2$ for a range of Co substitution at selected temperatures. Regardless of the doping concentration x, broad peaks associated with interband transitions appear for $\omega > 10\,000$ cm^{-1} (see the inset). For the lower frequency region, in contrast, the optical conductivity strongly depends both on doping and temperature. For $x > 0.3$ and $T > T^*$, similarly to other heavy fermion compounds [9, 10], the dependence on frequency of σ_1 can be described by a simple Drude model, $\sigma_1(\omega) = \sigma_{dc}/(1 + \omega^2\tau^2)$, where τ is the carrier relaxation time, which is a function of frequency (see the inset of figure 2). For $x = 1$, 0.6, and 0.5 the low $-T\sigma_1$ is suppressed with decreasing photon energy, showing a hump, which is marked by a arrow in figure 1, around 1600, 1500, and 1300 cm^{-1}, respectively. The optical conductivity at lower doping ($x \leqslant 3$), however, does not have hump structure and is almost independent of temperature. Figure 3 shows the real part of the dielectric constant $\epsilon_1(\omega)$ of $CeNi_{1-x}Co_xGe_2$. $\epsilon_1 = 0$ is found at near 17 700 cm^{-1}, which is almost independent on temperature and Co concentration (not shown). This value is called a plasma frequency of the bare conduction band screened by interband transitions. Below 100, 50, and 30 K for $x = 1$, 0.6,and 0.5, respectively, another plasmon is observed in the low frequency region of $\epsilon_1(\omega)$, marked by arrows in figure 3: 1150, 780, and 750 cm^{-1}. The frequency is independent of temperature within a error limit. In the quantum critical metal and antiferromagnet ($x \leqslant 0.3$), however, the low frequency plasmon is not observed even at the lowest temperature. The low frequency plasmon has been observed at low temperature in other heavy fermion compounds [9, 10]. The change of

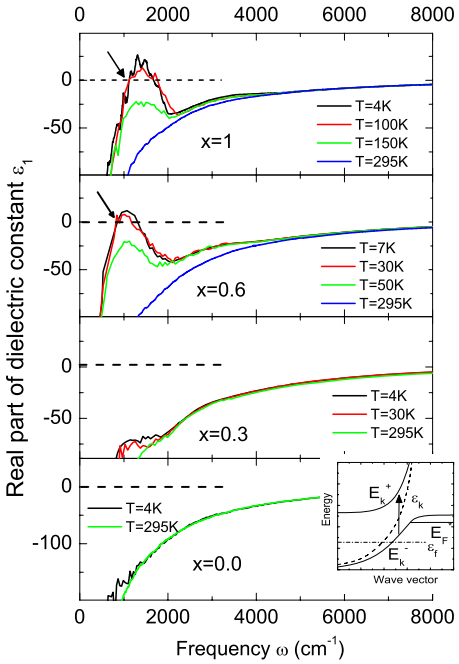

Figure 3. Real part of dielectric constant ϵ_1 of $CeNi_{1-x}Co_xGe_2$ ($x = 1.0$, 0.6, 0.3 and 0.0) for selected temperatures in the infrared region. The inset depicts a renormalized band structure calculated from a lattice Anderson model [14]. ϵ_k and ϵ_f denote bands of free carriers and localized f-electrons, respectively.

plasmon frequency corresponds with the change of carrier density and effective mass. Since a dramatic change in electrical resistivity is not observed below the temperature showing the reduction of plasmon frequency, observation of low frequency plasmon is due to heavy quasiparticles. Such a heavy quasiparticle has been qualitatively explained by the Anderson periodic lattice model. In this model, a band of conduction electrons is hybridized with localized 4f electrons below T^*, which is called the coherence temperature, leading to the dispersion relation schematically shown in the inset of figure 3. The hybridized band at the Fermi energy is flat, thus accounting for the renormalized scattering rate and effective mass at low temperatures [12–14]. The plasmon at high temperature is caused by electrons of bare conduction band, which is depicted by a dashed line in the inset of figure 3 and has a light band mass. According to this model, the temperature showing the low frequency plasmon corresponds to the coherence temperature. As shown in the inset, the gap in the density of states between hybridized bands opens below $T < T^*$ and can lead to interband transitions. Temperatures showing the hump and the low frequency plasmon are the same. These features strongly suggest that the hump is due to the hybridized gap. The coherence temperature T^* below which the electronic structure is reconstructed decreases with reducing x: it is 125, 40, and 22.5 K, as evaluated from the average value between the temperatures just below and above that at which the low frequency plasmon appears, for $x = 1$, 0.6, and 0.5, respectively.

Another consequence of hybridization in heavy fermion metals is enhancement of the effective mass (m^*), which is shows up as a narrow resonance near $\omega = 0$ in the optical

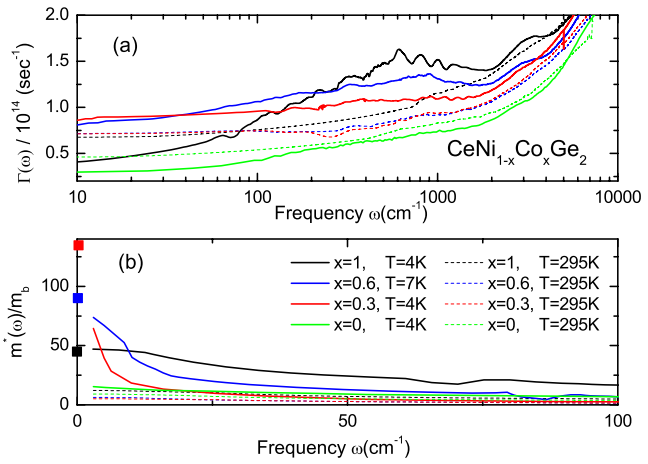

Figure 4. (a) Scattering rate Γ and (b) effective mass m^* of $CeNi_{1-x}Co_xGe_2$ ($x = 1$, 0.6, 0.3 and 0.0) at $T = 4$ and 295 K. Symbols on the left axis represent the effective mass evaluated from specific heat measurements.

conductivity [10]. Optical conductivity of $CeNi_{1-x}Co_xGe_2$ for $x > 0.3$ indeed reveals the expected narrow resonance in the coherence state: $\sigma_1(\omega)$ at the lowest measured frequency (60 cm^{-1}) agrees well with that of dc electrical resistivity for $T > T^*$, while dc resistivity is larger than the ac conductivity at $\omega = 60$ cm^{-1} for $T < T^*$, indicating narrow resonance (see the inset of figure 1). The renormalized scattering rate (Γ) of conduction electrons off heavy quasiparticles is described in the extended Drude model:

$$\Gamma(\omega) = \frac{\omega_P^2}{4\pi}\frac{\sigma_1}{|\sigma|^2} \tag{1}$$

and

$$\frac{m^*(\omega)}{m_b} = \frac{\omega_P^2}{4\pi}\frac{\sigma_2}{\omega|\sigma|^2}, \tag{2}$$

where m_b is the bare electron mass, σ_1 (σ_2) is the real (imaginary) part of optical conductivity σ and $\omega_P = (4\pi e^2 n/m_b)^{1/2}$ is the plasma frequency. Figures 4(a) and (b) display the scattering rate Γ and effective mass m^* of $CeNi_{1-x}Co_xGe_2$, which are estimated from this model. In the incoherence Kondo regime ($T > T^*$) for $x > 0.3$, Γ and m^* are nearly independent of photon energy, resembling a simple Drude behavior. In the coherence regime of the heavy Fermi state ($T < T^*$), in contrast, the scattering rate is suppressed near the hybridization gap ($\approx$1600 cm^{-1}), while the effective mass increases with decreasing frequency below the gap. For $x < 0.3$, where T^* is undetectable down to the lowest measuring temperature, however, Γ decreases monotonically with decreasing frequency without such a local minimum.

The effective mass, m^*/m_b, monotonically increases with decreasing ω at high temperature. The increase becomes steep below 10 cm^{-1} at low temperature for $x \geqslant 0.3$ and the effective mass tends to approach the value evaluated from specific heat measurements. In the calculation of the effective mass from the specific heat measurement, the carrier concentration is evaluated from the fitted plasma energy at 295 K mentioned above. In this evaluation the carrier concentration is assumed

to be independent of temperature. For $x = 0$, the mass enhancement in the antiferromagnetic state at $T = 4$ K is about two times compared to the value derived for $T = 295$ K. This increase ratio is significantly smaller than the ratio for the heavy fermion states ($x > 0.3$). The antiferromagnetic state comes from the RKKY interaction. The interaction is a indirect interaction between 4f electrons through the hybridization between 4f electrons and conduction electrons. The increase of mass enhancement seems mainly to be due to the magnetic excitations through the c–f hybridization. The c–f hybridization in the antiferromagnetic state does not form the renormalized band shown in the inset of figure 3. This result is consistent with the fact that the infrared hump is not observed at $x = 0$.

Direct evidence for non-Fermi liquid behavior near the quantum critical point comes from the scattering rate (Γ). In figure 2, Γ shows ω^2 dependence in the coherence state for $x > 0.3$, a hallmark of Fermi liquid behavior as is T^2 dependence in dc electrical resistivity. Figure 2 also shows the scattering rate at $x = 0.3$ and 4 K, i.e., in the quantum critical regime. Deviating from Fermi liquid ω^2 dependence, Γ follows an anomalous linear dependence on ω, that corresponds to a linear-T behavior in electrical resistivity. Disorder effects which are often connected to NFL behavior in nonstoichiometric compounds may be ruled out in this work because FL behavior is recovered at higher doping concentration ($x > 0.3$). The scattering rate at $x = 0$ and 4 K (antiferromagnetic regime) shows $\omega^{2.1}$ dependence, which corresponds to $T^{2.2}$ behavior in electrical resistivity. The deviation from the Fermi liquid behavior seems to be due to magnetic scattering.

One of the key issues in understanding quantum critical effects centers on the nature of 4f electrons near a QCP: in particular, whether the Kondo singlet forming temperature T_K remains finite or zero when the long-range magnetic ordering temperature T_N goes to zero [5]. If local moments are quenched at a finite temperature above the QCP, local moments do not play a role and the spin-density wave model must be used [4]. In this case, the continuity of the 4f electronic structure through QCP is warranted. If local moments are present at all temperatures down to $T = 0$ K at the QCP, the heavy electron Fermi surface and the coherence temperature will collapse at this point [5]: in the case of $T^* > 0$ the heavy electron Fermi surface exists below T^*, whereas in case of $T^* = 0$ (QCP) the 4f electronic structure will be kept down to 0 K. In Co-doped $CeNi_{1-x}Co_xGe_2$, the characteristic temperature T^* below which optical conductivity indicates formation of hybridization gap decreases progressively with decreasing Co concentration x and is undetectable down to the lowest measuring temperature (4 K) at the QCP ($x = 0.3$). As shown in figure 5, the optically determined coherence temperatures (T^*) are similar to those determined by electrical resistivity (T_R^*), i.e., the temperature at which the resistivity shows a maximum value [8]. The consistency between the two techniques shows that the coherence temperature is where the hybridization gap is indeed formed. Even though the present optical measurements are limited to 4 K at $x = 0.3$, we expect an absence of heavy quasiparticles down to zero temperature

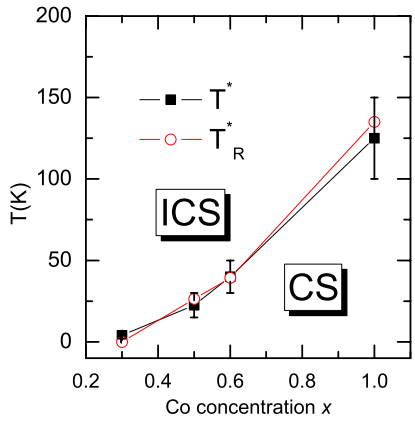

Figure 5. Coherence temperature T^* is defined as the average value between the temperatures just below and above that at which the low frequency plasmon appears. Error bars are temperature steps of the optical measurements. T_R^* is the temperature where electrical resistivity shows a maximum. CS and ICS mean the coherence state and incoherence state, respectively.

because T^* is completely suppressed, indicating the collapse of the heavy electron Fermi surface at this concentration ($x = 0.3$).

To summarize, the renormalized band formed by the hybridization below the coherence temperature (T^*) leads to a low frequency plasmon and the absorption hump in optical conductivity for $x > 0.3$ in $CeNi_{1-x}Co_xGe_2$. At $x = 0.3$, however, the coherence temperature extrapolates to zero temperature, indicating a lack of heavy quasiparticles at this magnetic QCP ($x = 0.3$). The fact that the heavy electronic state ceases to exist at $x = 0.3$, where the long-range magnetic order is completely suppressed, indicates that locally critical magnetic fluctuations are responsible for the non-Fermi liquid behavior in this compound.

Acknowledgments

This work is supported by the Korea Science and Engineering Foundation through the Center for Strongly Correlated Materials Research (CSCMR) at Seoul National University, by grant No. R01-2003-000-10095-0 from the Basic Research Program of the Korea Science and Engineering Foundation, and by Korea Research Foundation through Grant No. KRF-2005-070-C00044, and is performed for the Nuclear R&D Programs funded by the Ministry of Science and Technology (MOST) of Korea.

References

[1] Coleman P and Schofield A J 2005 *Nature* **433** 226
[2] Park T, Ronning F, Yuan H Q, Salamon M B, Movshovich R, Sarrao J L and Thompson J D 2006 *Nature* **440** 65
[3] Schröder A, Aeppli G, Coldea R, Adams M, Stockert O, Löhneysen H v, Bucher E, Ramazashvili R and Coleman P 2000 *Nature* **407** 351
[4] Hertz A J 1976 *Phys. Rev.* B **14** 1165
Millis A J 1993 *Phys. Rev.* B **48** 7183
[5] Si Q, Rabello S, Ingersent K and Smith J L 2001 *Nature* **413** 804

Coleman P, Pepin C, Si Q and Ramazashvili R 2001 *J. Phys.: Condens. Matter* **13** R723
[6] Paschen S, Lühmann T, Wirth S, Gegenwart P, Trovarelli O, Geibel C, Steglich F, Coleman P and Si Q 2004 *Nature* **432** 881
[7] Shishido H, Settai R, Harima H and Onuki Y 2005 *J. Phys. Soc. Japan* **74** 1103
[8] Lee B K, Hong J B, Kim J W, Jang K-H, Mun E D, Jung M H, Kimura S, Park T, Park J-G and Kwon Y S 2005 *Phys. Rev.* B **71** 214433
[9] Dordevic S V, Basov D N, Dilley N R, Bauer E D and Maple M B 2001 *Phys. Rev. Lett.* **86** 684
[10] Degiorgi L 1999 *Rev. Mod. Phys.* **71** 687
[11] Coleman P 1987 *Phys. Rev. Lett.* **59** 1026
[12] Millis A J and Lee P A 1987 *Phys. Rev.* B **35** 3394
Millis A J *et al* 1987 *Phys. Rev.* B **36** 864
[13] Fulde P 1993 *Electron Correlations in Molecules and Solids* 2nd edn (Berlin: Springer)
[14] Hewson A C 1997 *The Kondo Problem to Heavy Fermions* (Cambridge: Cambridge University Press)